

Numerical study of the noise power of a carbon nanowire networkChenggang Zhou¹ and X.-G. Zhang^{1,2}¹*Center for Nanophase Materials Sciences, Oak Ridge National Laboratory, P.O. Box 2008, Oak Ridge, Tennessee 37831-6493, USA*²*Computer Science and Mathematics Division, Oak Ridge National Laboratory, P.O. Box 2008,**Oak Ridge, Tennessee 37831-6493, USA*

(Received 29 May 2008; published 18 November 2008)

A thin film made of a carbon nanowire network can be mapped into a resistor network containing tunnel junctions that are randomly switched. In such a network the variance in individual resistance is infinity so the perturbative analysis must be applied on conductances. We study the relationship between the noise power and the network morphology through a Monte Carlo simulation of the conductance and the $1/f$ noise spectrum. We find that the noise power scales with the average current in a power law $S \propto I^{-\omega}$, where ω is a function of the network morphology. The noise spectrum is studied in detail, and we give a simple explanation for the observed relation between total noise power and the conductance.

DOI: [10.1103/PhysRevB.78.174307](https://doi.org/10.1103/PhysRevB.78.174307)

PACS number(s): 73.50.Td, 73.63.Fg, 05.10.Ln, 05.40.Ca

I. INTRODUCTION

Random resistor networks are often used to model percolation-type transport in a wide range of physical problems. Early examples of using low-frequency resistance fluctuations to study charge transport in disordered solids were reviewed by Dutta and Horn¹ and by Weissman.² More recent examples include the study of mixed phase materials in two dimensions (2D) (Ref. 3) and three dimensions (3D),⁴ amorphous materials,⁵ and conducting polymers.⁶ For these random resistor networks, noise power measurement can often reveal more information than a simple dc measurement.

The scaling exponents of the noise power with respect to the total dc voltage or the total measured resistance are expected to vary with the network morphology. However, there has not been a study to connect the scaling exponents with a quantifiable network characteristics that can be compared to experimental measurements. The knowledge of such connections would be highly desired if we wish to use noise measurement as a probe of physical processes in disordered media. Furthermore, most studies are focused on scaling characteristics of the networks close to the percolation threshold, whereas most useful applications are in the regime far away from the percolation threshold.

Here we report an attempt to quantify a simple network far away from the percolation threshold and to connect its characteristics to the scaling exponents of the noise power. Our model is motivated by recent works^{7,8} on thin films of carbon nanotubes and carbon nanowires (CNWs), used as transparent electrodes to enhance the efficiency of organic light-emitting diode (OLED). Under a microscope, these films appear to be random networks of CNWs of different lengths and bundle sizes. Properties of the film depend on its thickness, as well as average size of the CNWs and the geometry of the random network.

The resistance of the CNW film comes from the resistance of CNWs and the junction resistance between touching CNWs. The CNWs consist of bundles of multiwall nanotubes of different diameters. Due to the disorder and impurities in the nanowires, they behave as Ohmic resistances at room temperature.⁹ Besides the junctions of CNWs, where

two CNWs touch, there are also branching points where a thick CNW separates into several thinner ones. At low temperatures, the junctions between single-walled carbon nanotubes exhibit different I - V curves depending on whether the touching nanotubes are metallic or semiconducting.^{10,11} Both diode behavior and power-law I - V curve of Luttinger liquid have been observed. At room temperature, the nonlinearity in the I - V curves are much less pronounced. Since CNWs contain many multiwalled nanotubes, a junction between two CNWs are likely to contain several touching points between individual nanotubes. It is reasonable to model each junction with a temperature-dependent resistor. In addition, $1/f$ noise has been observed in similar nanotube networks.⁸ It has been suggested that the noise analysis could be a tool to characterize and investigate the internal structures of the film.

II. CONSTRUCTION OF THE NETWORK CONFIGURATION

The CNW film is a complex system with a lot of physical processes contributing to its macroscopic properties. A microscopic model that contains every detail of its building blocks is prohibitively complicated. In order to study these films, we try to capture the main ingredients responsible for charge transport with a simple random network model.

One can use dynamic Monte Carlo simulations to simulate the deposition of CNWs on to the substrate, forming a random network. This approach is computationally demanding. To generate the random network quickly, we use a less complicated method. We randomly place junctions in the first step of the construction and then connect these junctions with straight lines representing CNWs. The film in the model is defined in a rectangular area $L_x \times L_y$ and has a small thickness L_z . In the simulations presented here, we have typically used $L_x=5 \mu\text{m}$, $L_y=4 \mu\text{m}$, and $L_z=0.1 \mu\text{m}$. The units are of no importance in our simulations because they can always be rescaled to fit the experimental value if necessary. We apply periodic boundary condition in the y direction and open boundary conditions in the other two directions. The number of junctions in this area, N , was varied from 300 to 1500 in the simulations. The connectivity c , defined as the

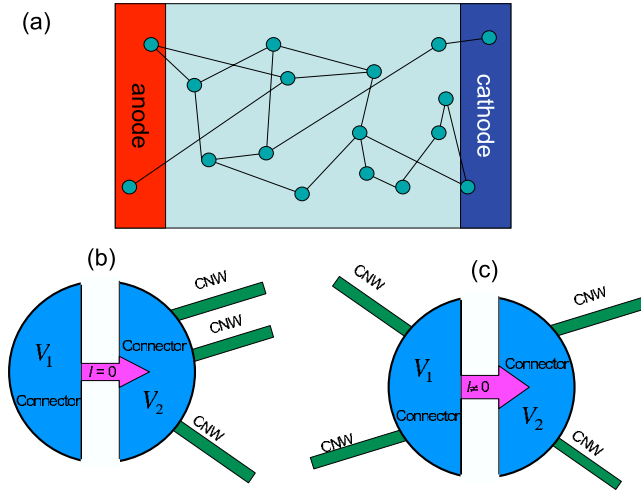


FIG. 1. (Color online) A schematic drawing of the random network model and the internal structure of junctions. (a) The entire network consists of junctions connected by CNWs, anode, and cathode, (b) typical branching junction, and (c) typical touching junction with CNWs connected to both connectors.

average coordination number, is an important parameter, which determines the number of CNWs N_W that we are going to draw between junctions. Since every wire is connected to two junctions, $N_W = Nc/2$. We also impose a cutoff of the length of CNWs L_{\max} , which is set at $0.5 \mu\text{m}$ in the simulations. To insert a CNW, we randomly pick two junctions. If their distance is larger than L_{\max} , they are discarded and another pair is picked; otherwise, they are connected.

As we mentioned, the junctions can be branching points or touching points; therefore they have internal structures. We define two connectors inside each junction, which have different voltages as shown in Fig. 1. When we attach a CNW to a junction, we randomly choose one of the connectors. The wires connected to the same connector are treated as being on the same CNW. If there are two CNWs connected to the same connector, they represent a single continuous CNW; if there are more than two, this connector represents a branching point. CNWs connected to different connectors on the same junction are considered as touching each other. Since two connectors on the same junction may have different voltages, a current between them is determined by a given I - V curve of the junction. Finally, the resistances on the CNWs are calculated and saved. For simplicity, we assume their resistances are given by $R = \rho L$, where ρ is a constant resistance per unit length and L is the length of the CNW.

The state of the network is specified by the voltages on the connectors, two for each junction. The current on each CNW and through each junction is a function of these voltages. To simulate the electric transport, we define the anode and cathode on the film. The anode extends from $x=0$ to $0.5 \mu\text{m}$, and cathode extends from $x=L_x - 0.5 \mu\text{m}$ to L_x . All junctions in the anode have fixed voltage at $V > 0$, and all the junctions in the cathode have their voltages fixed at zero. In a steady state, the current distribution is “divergence free,” i.e., there is no charge accumulation or depletion on each of the connectors;

$$\frac{dQ_{i,\sigma}}{dt} = \sum_{j,\delta} I(j,\delta;i,\sigma) = 0. \quad (1)$$

Here the subscripts i and σ label the junction and one of the two connectors in this junction. If the junctions have fixed resistance, the current $I(j,\delta;i,\sigma)$ in the above equations always have the form,

$$I(j,\delta;i,\sigma) = \frac{V(i,\sigma) - V(j,\delta)}{R(i,\sigma;j,\delta)}, \quad (2)$$

and the linear equations of Eq. (1) can be solved efficiently. In particular, we have used the LU decomposition¹² to solve these linear equations. One frequently appearing special case is nodes disconnected from both the anode and the cathode. The voltages on these nodes remain undetermined and their corresponding diagonal matrix elements in the U matrix (upper triangular) are zero. Thus, after the LU decomposition, the lines and columns in the U matrix corresponding to zero diagonal matrix elements can be deleted because they correspond to disconnected junctions. The voltages on the remaining junctions can be solved with the standard Gaussian reduction algorithm. The disconnected junctions can have arbitrary values of voltage. A by-product from this algorithm is the number of junctions that participate in the conduction.

If the junctions have nonlinear I - V curves, it is intuitive that a steady state must exist, but the uniqueness of the steady state is not guaranteed. In order to find a steady state, a simple method we have used is to simulate the charging process of hypothetical capacitances on the connectors. To implement this we assume all the connectors have capacitance C , then Eq. (1) becomes

$$\frac{dV_{i,\sigma}}{dt} = C^{-1} \sum_{j,\delta} I(j,\delta;i,\sigma), \quad (3)$$

where $I(j,\delta;i,\sigma)$ is a function of $V_{j,\delta}$ and $V_{i,\sigma}$. This group of differential equations are solved numerically to find a steady state. C is not necessarily a constant. It can be tuned during the calculation to accelerate the convergence.

III. NOISE SPECTRUM SIMULATION

It was found by Soliveres *et al.*,⁸ Snow *et al.*,¹³ and Collins *et al.*¹⁴ that carbon nanotubes and their random network exhibit much larger electric noise than metals and semiconductors. Typical $1/f$ noise spectrum has been observed in both electrical current and conductivity. We expect the strong $1/f$ noise to come from two sources: first the intrinsic noise from conduction inside CNWs, which is related to the impurities and defects there, and second the microscopic random structure of the network, which is related to the conduction through junctions. We are particularly interested in the second kind of noise; so the next step in our simulation is to generate a $1/f$ noise and compare it to the experiment.

According to the McWhorter¹⁵ model of the $1/f$ noises in electronic devices, the source of the noise is trapping sites of various relaxation times. The noise power spectrum of individual site is of Lorentzian form.² The $1/f$ noise spectrum results from the superposition of a large number of Lorentz-

ian spectra. An obvious way for the random structure of the film to contribute to the noise is to host unstable junctions between CNWs. A possible mechanism for the instability of the junctions is local trapping sites, whose occupation number affects the junction resistance. These local trapping sites randomly trap charge carriers near the junction and act as the trapping sites in the original McWhorter model.

We have followed the McWhorter model to simulate the noise spectrum in CNW random networks. The details of the local trapping sites or any other possible mechanism is not important. We only need to model the instability of the junctions. We select some junctions in our existing static model to be unstable junctions, which are allowed to exist in two states (on or off). In the on state, it has a constant resistance, while in the off state, its resistance is infinite. Each unstable junction switches between two states randomly and independently. According to the McWhorter model, the number of switches n_s in a unit time interval $[0,1)$ has a distribution proportional to $1/n_s$. We assume n_s ranges from 1 to a high-frequency cutoff of 4000. The cut-off frequency is associated with the fastest speed that a carrier can be emitted or absorbed, or in our mode, a connector can switch between two states. Because of the finite amount of memory on a computer, the cutoff is also necessary for the simulation. At the beginning of each simulation, we select a fraction p of junctions to be unstable; for every unstable junction we generate a time series of states in the following manner: pick n_s according to its distribution, then pick n_s random switching times $0 < t_1 < \dots < t_{n_s} < 1$, and a random initial state at $t=0$. In the subsequent calculation, the state of the network at any time in the interval $[0,1)$ is determined. When this is done, a time series of current is ready to be calculated, which is transformed into the frequency space by fast Fourier transform (FFT) to obtain its noise spectrum. The calculations are performed with a fixed voltage of 1 V between the anode and the cathode. Therefore the calculated current is equivalent to the conductance.

A. Simulated 1/f spectrum

Figure 2 shows the a noise spectrum from one of the simulations with $c=3$, $p=0.5$, and 1000 junctions. The junction resistance R_j is set at 100 kΩ and the CNW resistivity is set at 6 kΩ/μm. For this sample, $I(t)$ is calculated at 4096 different t values: $t_i=(i-1)/2^{12}$ in a normalized interval of time $[0,1)$. The time series $I(t_i)$ is transformed by FFT into the frequency domain. The transformed signal has complex amplitudes A_f at 2049 frequencies. The power spectrum is $S(f)=|A_f|^2$ by definition. Figure 2 shows the un-normalized $S(f)$ on 2048 nonzero frequencies. The raw data has a wide distribution at large frequencies; most data points fall between two straight lines $10/f$ and $10/f^2$. After performing a moving average, $S(f)$ with large values are dominating the average power spectrum. As shown in Fig. 2, the red curve after moving average closely follows the dashed line $10/f$. This curve is extremely similar to the experimental result⁸ because the moving average is a simple filter in the frequency domain, while the experimental measurement of spectrum power nevertheless uses certain filter in signal processing.

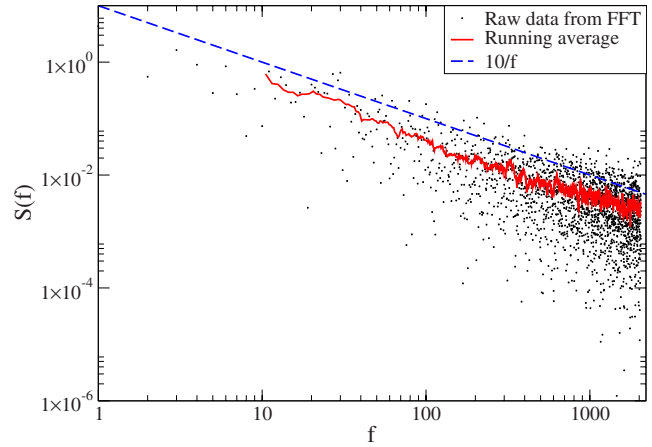


FIG. 2. (Color online) A typical 1/f noise spectrum from the simulation. The raw data from FFT contains data for totally 2048 nonzero frequencies for a time series of length 4096. After moving average over adjacent 20 data points, the red solid curve is very similar to the experimental result in Ref. 8. The unit of $S(f)$ as plotted is $(mA)^2$. The dashed line is a guide for the eyes.

We have performed simulations for systems with $c=3, 4$, $p=0.25, 0.5, 0.75$, and 1, and $N=300-1500$. The 1/f spectrum has been observed in all the simulations.

B. Total noise power and its scaling with the current

The total noise power is calculated as

$$S = \frac{1}{M} \sum_{i=1}^M [I(t_i) - \langle I \rangle_t]^2, \tag{4}$$

where $\langle I \rangle_t$ is the time-averaged current in the simulation. Because the unstable junctions switch between two states and the probability of being in one of the two states is 1/2, the probability for the system to be in any state labeled by (s_1, \dots, s_{N_u}) is simply 2^{-N_u} , which is also the expected length of time for the system to be in this state in a unit time interval. Consider the current I as a function of the configuration of the network which is specified by the states of all the unstable junctions $\{s_1, s_2, \dots, s_{N_u}\}$, then

$$\langle I \rangle_t = 2^{-N_u} \sum_{s_1, \dots, s_{N_u}} I(s_1, \dots, s_{N_u}), \tag{5}$$

$$S = 2^{-N_u} \sum_{s_1, \dots, s_{N_u}} I^2(s_1, \dots, s_{N_u}) - \langle I \rangle_t^2, \tag{6}$$

which is a result of the ergodicity of the simulation. The choice of the distribution of the relaxation time does not affect the total noise power, at least in the lowest order of approximation. It can only redistribute some noise power from one frequency to another. The total noise power is determined by static properties such as number and distribution of the unstable junctions and independent of their relaxation times.

We have calculated the total noise power for a large number of samples. Figure 3 plots pairs (I, S) from simulations

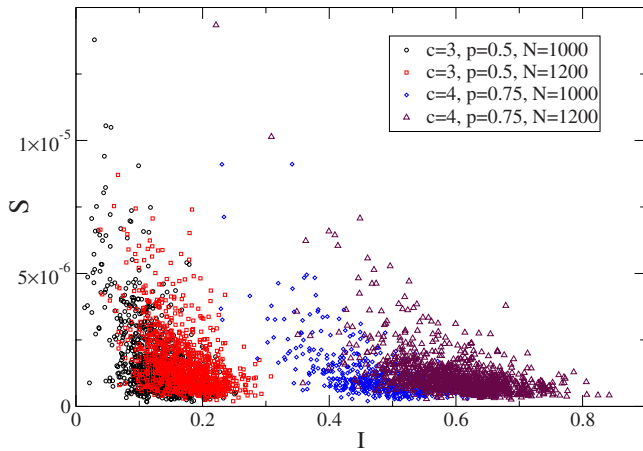


FIG. 3. (Color online) Noise power vs average current from simulations of different connectivity, fraction of unstable junctions, and number of junctions. Each group contains 1000 samples. The simulations were performed with the same fixed voltage; therefore the current is proportional to the conductance.

with different connectivity and number of junctions.

The overall trend of the noise power in Fig. 3 is expected, which decreases with increasing current. Since the average current indicates, roughly, the average number of path that a charge can go from anode to cathode, the more path a sample has, the more robust it is against the fluctuation of individual junctions.

To be more quantitative, we divided the range of I into ten windows for each group of data and calculated the average current and noise power in each window of current. The result is shown in Fig. 4. The error bars of first and last few data points in each data set in Fig. 4 are relatively large because there are fewer sample points at the tails of the distribution of current, as shown in Fig. 3. The middle data points in Fig. 4 follow closely the power law,

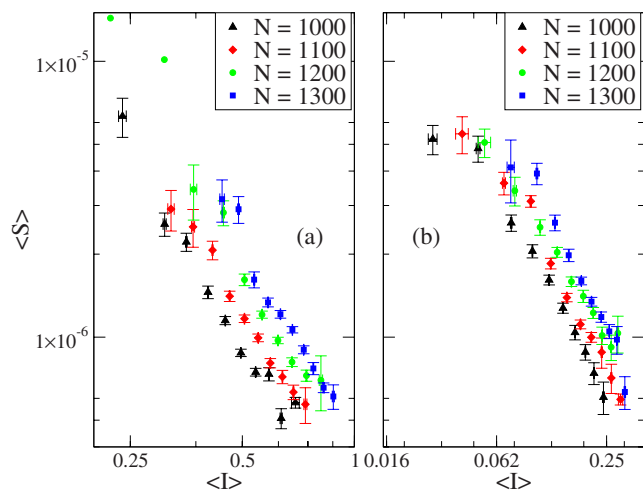


FIG. 4. (Color online) Relationship between average noise power and current. (a) $c=4$ and $p=0.75$ and (b) $c=3$ and $p=0.5$, indicates $\langle S \rangle / \sqrt{N} \propto (\langle I \rangle / N)^{-\omega}$, where ω is independent of the CNW density which is proportional to N .

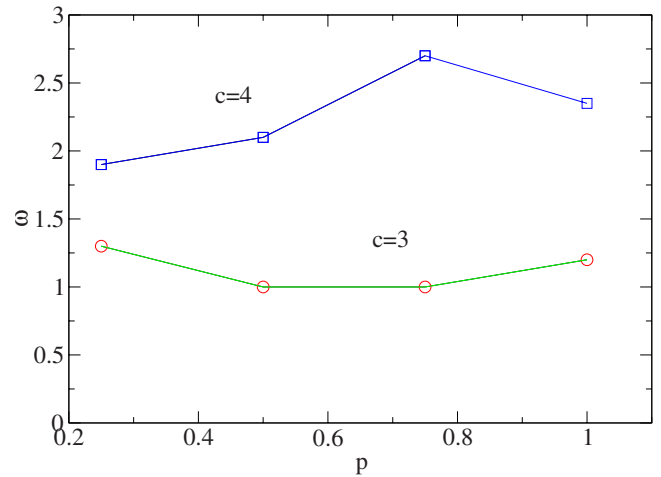


FIG. 5. (Color online) Scaling exponent ω depends on both c and p and can be a good measure of the network morphology.

$$\frac{S}{\sqrt{N}} \propto \left(\frac{\langle I \rangle}{N} \right)^{-\omega}. \quad (7)$$

The exponent ω is found to be independent of the number of junctions, N . Close to the percolation threshold, N may scale with a very high power of the CNW density. In our case, however, far away from the percolation threshold, N is approximately proportional to the CNW density. Therefore our results cannot be compared to measurements close to the percolation threshold. New experiments are needed to be designed to compare them with these results.

In Fig. 5, we show the dependence of the scaling exponent ω with respect to both c and p . The dependence on p is nonmonotonic. ω is more than doubled when c is changed from 3 to 4. Therefore measurement of ω can be used to analyze the network morphology.

C. Noise power scaling with the junction resistance

In order to extract more information on the correlation between geometrical disorder and current noise, we studied the relation between the noise power and the junction resistance. In reality, the junction resistance might be a tunable parameter, for example, that can be changed with the applied voltage or temperature. We expanded the simulations to repeat the calculation of current and noise with different junction resistances. Typically, we have used $R_j=50, 100, \dots, 500$. Figure 6 shows $I(t)$ calculated with different junction resistances for a typical sample.

When R_j is small, the fluctuation in $I(t)$ is large because the extra conductance that the network obtains from switching on a junction is larger when the resistance of the junction is small. When R_j becomes large enough, the current almost entirely flows in the fixed part of the network no matter whether the unstable junctions are on or off. Different sequences of $I(t)$ are also very similar. Indeed, their correlation is close to 1. This is because they are generated by the same sequence of network configurations in time. We have also found that the histogram of $I(t)$ can always be fitted with a Gaussian distribution no matter what value is used for R_j .

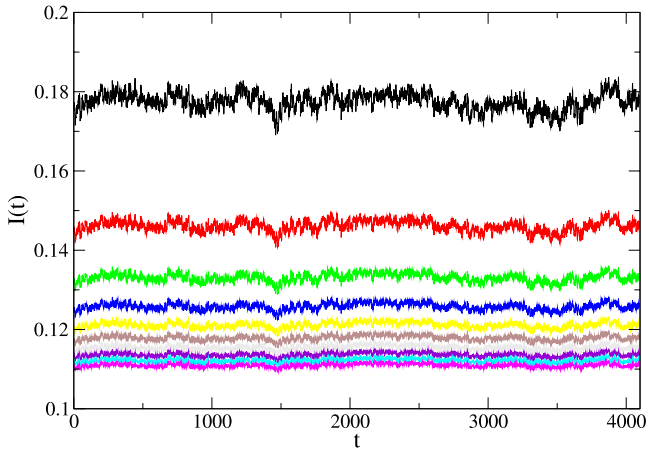


FIG. 6. (Color online) The time series $I(t)$ for a sample with different junction resistances. From top to bottom, $R_j=50, 100, \dots, 500$ k Ω .

Since we did not start with any Gaussian distributions, this is a hint that the noise in (t) can be explained in terms of a large number of independent random variables.

Consider that a network configuration is reached by turning on junctions one by one starting from the fixed part of the network. Every time a junction is turned on, there is a small increment in the current;

$$x_i = \delta I = I(\dots, s_{j_i} = 1, \dots) - I(\dots, s_{j_i} = 0, \dots). \quad (8)$$

This increment is a small random number. A single junction is always a small perturbation to the entire network as we can see from $I(t)$ that the amplitude of its fluctuation, which is contributed by many unstable junctions, is never larger than 10% of its average value. Thus, it is reasonable to assume that after a junction is turned on, the network is still in the same statistical ensemble. The next junction to be turned on will lead to x_{i+1} , which will have the same distribution function as x_i . So now the current can be written as

$$I = I_0 + \sum_{i=1}^k x_i, \quad (9)$$

where I_0 is the current of the fixed part of the network. Notice k is also a random variable because the unstable junctions are switched on independently with probability 1/2. We assume x_i 's are independent identically distributed random variables. Then, it follows from the Wald identity that

$$\mathbb{E}(I) = I_0 + \mathbb{E}(k)\mathbb{E}(x_i), \quad (10)$$

where the expectation of k is based on a binomial probability distribution, and the expectation of x_i can be in principle calculated with the probability distribution of x_i . The noise power can be calculated similarly,

$$S = \text{var}(I) = \text{var}(k)[\mathbb{E}(x_i)]^2 + \text{var}(x_i)\mathbb{E}(k). \quad (11)$$

When we reduce the junction resistance R_j , the distribution of x_i extends to larger values, which results in changes in $\mathbb{E}(x_i)$ and $\text{var}(x_i)$. However, the expectation and variance of k are constants. The noise power can be further expressed as

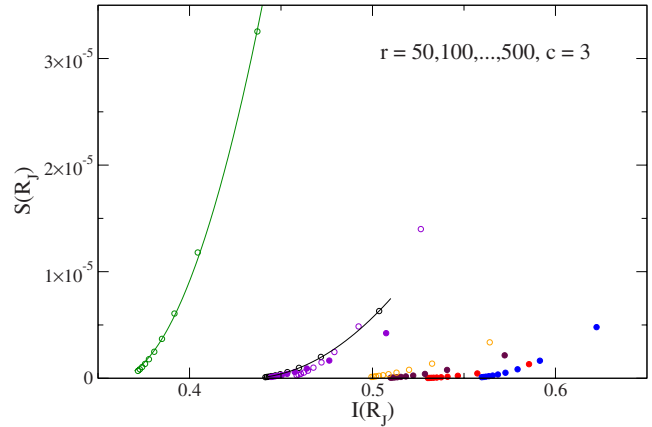


FIG. 7. (Color online) Parametric plot of $S(R_j)$ vs $I(R_j)$ for several samples with varying R_j . The solid lines are quadratic fits of two of the data sets.

$$S = A[\mathbb{E}(I) - I_0]^2 + B[\mathbb{E}(I) - I_0], \quad (12)$$

where $A = \text{var}(k)/[\mathbb{E}(k)]^2$ and $B = \text{var}(x_i)/\mathbb{E}(x_i)$. Furthermore, since k has a binomial distribution, $A = 1/N_u$, where N_u is the number of unstable junctions. The distribution function of x_i is expected to be similar to a Γ distribution, a change in R_j most likely results in a rescaling of x_i . Based on dimensional analysis, we expect B and $\mathbb{E}(x_i)$ is of the same order. Therefore, the relation between S and $I - I_0$ should be dominated by a quadratic function with a possible small linear term. The physical meaning of the coefficient A and I_0 have already been explained. This simple relation is illustrated in Fig. 7. According to the analysis above, to the lowest order, the fluctuation is a result of number fluctuation of the conducting junctions, while $\mathbb{E}(x_i)$, determined by R_j , only enters as a scaling factor.

IV. CONCLUSIONS

The average conductance calculated from static model does not give us any surprise. Except when the connectivity is very low, such as $c=2$, the model CNW film behave as a regular conducting film, which is expected. It is obvious that with a given amount of CNWs, one should increase the connectivity to increase the conductivity of the film. In the simulation of the noise spectrum, we have made a few assumptions. First, we are interested in the noise coming from the junctions between CNWs only. Second, the junction resistance is a constant. We expect the real noise will be larger than what the simulations have produced because there are also intrinsic noise in the CNWs. However, the second assumption can be relaxed. As we have argued that the noise largely comes from the fluctuation in the number of conducting junctions. As long as $x_i = \Delta I$ can be approximated as independent identical random numbers, our analysis holds. The randomness in x_i can come both from the network structure or the random distribution of junction resistance. So we expect the $1/f$ spectrum and quadratic relation between current and total noise power hold if the junction resistance has a random distribution.

In the end, we have found that the total noise power and its relation to the current and junction resistance are most useful macroscopic quantities that contain information of the microscopic geometric structure of the CNW network. From the coefficient $A=1/N_u$, one can determine the fraction of unstable junction p since the total density of junctions can be estimated from microscope photographs of the CNW network. Furthermore, the exponent ω is determined by the connectivity of the random network c along with p . This is probably a feasible approach to assess the quality and the microscopic structure of CNW networks experimentally.

We also expect the random network model that we have

used is applicable to other problem in condensed-matter physics or subjects that involve large random network, where transport noise may be an important factor.

ACKNOWLEDGMENTS

This research at Oak Ridge National Laboratory's Center for Nanophase Materials Sciences was sponsored by the Assistant Secretary for Energy Efficiency and Renewable Energy, Office of Building Technology, U.S. Department of Energy, and by the Scientific User Facilities Division, Office of Basic Energy Sciences, U.S. Department of Energy.

¹P. Dutta and P. M. Horn, *Rev. Mod. Phys.* **53**, 497 (1981).

²M. B. Weissman, *Rev. Mod. Phys.* **60**, 537 (1988).

³Yigal Meir, *Phys. Rev. Lett.* **83**, 3506 (1999).

⁴Matthias Mayr, Adriana Moreo, Jose A. Vergés, Jeanette Arispe, Adrian Feiguin, and Elbio Dagotto, *Phys. Rev. Lett.* **86**, 135 (2001).

⁵Lisa M. Lust and J. Kakalios, *Phys. Rev. Lett.* **75**, 2192 (1995).

⁶J. S. Andrade, Jr., N. Ito, and Y. Shibusa, *Phys. Rev. B* **54**, 3910 (1996).

⁷Mei Zhang, Shaoli Fang, Anvar A. Zakhidov, Sergey B. Lee, Ali E. Aliev, Christopher D. Williams, Ken R. Atkinson, and Ray H. Baughman, *Science* **309**, 1215 (2005).

⁸S. Soliveres, J. Gyani, C. Delseny, A. Hoffmann, and F. Pascal, *Appl. Phys. Lett.* **90**, 082107 (2007).

⁹M. Bockrath, D. H. Cobden, P. L. McEuen, N. G. Chopra, A.

Zetti, A. Thess, and R. E. Smalley, *Science* **275**, 1922 (1997).

¹⁰M. S. Fuhrer, J. Nygard, L. Shih, M. Forero, Y.-G. Yoon, M. S. C. Mazzoni, H. J. Choi, J. Ihm, S. G. Louie, A. Zetti, and P. L. McEuen, *Science* **288**, 494 (2000).

¹¹Z. Yao, H. W. Ch. Postma, L. Balents, and C. Dekker, *Nature (London)* **402**, 273 (1999).

¹²Roger A. Horn and Charles R. Johnson, *Matrix Analysis* (Cambridge University Press, Cambridge, 1985), Sec. 3.5.

¹³E. S. Snow, J. P. Novak, M. D. Lay, and F. K. Perkins, *Appl. Phys. Lett.* **85**, 4172 (2004).

¹⁴Philip G. Collins, M. S. Fuhrer, and A. Zettl, *Appl. Phys. Lett.* **76**, 894 (2000).

¹⁵A. L. McWhorter, in *Semiconductor Surface Physics*, edited by R. H. Kingston (University of Pennsylvania, Philadelphia, 1957).